

# PDGFR $\beta$ -positive cell-mediated post-stroke remodeling of fibronectin and laminin $\alpha$ 2 for tissue repair and functional recovery

Tomoya Shibahara<sup>1</sup>, Kuniyuki Nakamura<sup>1</sup>, Yoshinobu Wakisaka<sup>1</sup>, Masahiro Shijo<sup>2</sup> , Kei Yamanaka<sup>1</sup>, Masamitsu Takashima<sup>1</sup>, Hayato Takaki<sup>1</sup>, Masaoki Hidaka<sup>1</sup>, Takanari Kitazono<sup>1</sup> and Tetsuro Ago<sup>1</sup> 

## Abstract

Post-stroke intra-infarct repair promotes peri-infarct neural reorganization leading to functional recovery. Herein, we examined the remodeling of extracellular matrix proteins (ECM) that constitute the intact basal membrane after permanent middle cerebral artery occlusion (pMCAO) in mice. Among ECM, collagen type IV remained localized on small vessel walls surrounding CD31-positive endothelial cells within infarct areas. Fibronectin was gradually deposited from peri-infarct areas to the ischemic core, in parallel with the accumulation of PDGFR $\beta$ -positive cells. Cultured PDGFR $\beta$ -positive pericytes produced fibronectin, which was enhanced by the treatment with PDGF-BB. Intra-infarct deposition of fibronectin was significantly attenuated in pericyte-deficient *Pdgfrb*<sup>+/-</sup> mice. Phagocytic activity of macrophages against myelin debris was significantly enhanced on fibronectin-coated dishes. In contrast, laminin  $\alpha$ 2, produced by GFAP- and aquaporin 4-positive astrocytes, accumulated strongly in the boundary of peri-infarct areas. Pericyte-conditioned medium increased the expression of laminin  $\alpha$ 2 in cultured astrocytes, partly through TGF $\beta$ 1. Laminin  $\alpha$ 2 increased the differentiation of oligodendrocyte precursor cells into oligodendrocytes and the expression of myelin-associated proteins. Peri-infarct deposition of laminin  $\alpha$ 2 was significantly reduced in *Pdgfrb*<sup>+/-</sup> mice, with attenuated oligodendrogenesis in peri-infarct areas. Collectively, intra-infarct PDGFR $\beta$ -positive cells may orchestrate post-stroke remodeling of key ECM that create optimal environments promoting clearance of myelin debris and peri-infarct oligodendrogenesis.

## Keywords

Fibronectin, functional recovery, ischemic stroke, laminin  $\alpha$ 2, pericyte

Received 27 January 2022; Revised 3 October 2022; Accepted 1 November 2022

## Introduction

Reperfusion therapy with intravenous administration of recombinant tissue-plasminogen activator or catheter-mediated endovascular thrombectomy has been established as the most effective neuroprotective and neurorestorative therapy for acute ischemic stroke.<sup>1,2</sup> A potential therapeutic target for acute ischemic stroke is enhancement of neurorestoration with endogenous functional recovery during subacute phase. Although functional recovery occurs with rehabilitative therapy in most stroke patients until approximately 3 months after onset, its extent varies among individuals with comparable infarct size and

localization. Evidence suggests that macrophage-mediated clearance of intra-infarct debris is an important factor promoting post-stroke functional

<sup>1</sup>Department of Medicine and Clinical Science, Graduate School of Medical Sciences, Kyushu University, Fukuoka, Japan

<sup>2</sup>Department of Internal Medicine, Fukuoka Dental College Medical and Dental Hospital, Fukuoka, Japan

### Corresponding author:

Tetsuro Ago, Department of Medicine and Clinical Science, Graduate School of Medical Sciences, Kyushu University, 3-1-1 Maidashi, Higashi-ku, Fukuoka 812-8582, Japan.

Email: ago.tetsuro.544@m.kyushu-u.ac.jp

recovery.<sup>3,4</sup> We have demonstrated that microvascular platelet-derived growth factor receptor  $\beta$  (PDGFR $\beta$ )-positive pericytes crucially participate in post-stroke restoration of blood flow and subsequent recruitment of monocytes/macrophages within infarct areas through the production of chemokines such as monocyte chemoattractant protein-1 (MCP1)/C-C motif chemokine ligand 2 (CCL2).<sup>3</sup> Recruited macrophages remove myelin debris (MD) with the aid of neighboring pericytes, while promoting intra-infarct fibrotic responses mediated by PDGFR $\beta$ -positive cells. The clearance of debris and tissue repair within infarct areas, achieved by the close interaction of pericytes and macrophages, enhances peri-infarct neural reorganization, including astrogliosis and oligodendrogenesis, facilitating functional recovery.<sup>3,5-7</sup> Thus, creation of an optimal environment to support these intercellular interactions and functions in intra-infarct and peri-infarct areas is necessary to promote post-stroke functional recovery.

Extracellular matrix proteins (ECM) can modulate cellular functions through direct interaction with adhesive molecules expressed on cellular membranes.<sup>8</sup> In the brain, endothelial cells, pericytes, and astrocytes produce ECM, such as collagens, laminins, fibronectin, and perlecan, and constitute the basal membrane (BM), a crucial component of the blood-brain barrier (BBB).<sup>9-12</sup> Since BBB is disrupted by degradation of ECM in ischemic areas, they have to be suitably remodeled to promote tissue repair and functional recovery.<sup>13,14</sup> However, it is not clear how the production of ECM is regulated after acute ischemic stroke for post-stroke tissue repair and functional recovery.<sup>14</sup> In this study, we examined the remodeling of ECM and their roles in tissue repair and functional recovery using a permanent middle cerebral artery occlusion (pMCAO) model in mice.

## Materials and methods

### Animals

Animal experiments were conducted in accordance with the Guidelines for Proper Conduct of Animal Experiments by the Science Council of Japan (June 1, 2006) (<http://www.scj.go.jp/ja/info/kohyo/pdf/kohyo-20-k16-2e.pdf>). The Animal Care and Use Review Committee of Kyushu University approved the experimental procedures (Fukuoka, Japan) (A29-153) and the study has been reported according to the ARRIVE guidelines.<sup>3</sup> 129S *Pdgfrb*<sup>+/-</sup> mice were purchased from Jackson Laboratory (Bar Harbor, ME, USA; <https://www.jax.org/strain/007846>) and were backcrossed ten times with C57BL/6 mice to produce C57BL/6 *Pdgfrb*<sup>+/-</sup> mice.<sup>5</sup> We used male and female

*Pdgfrb*<sup>+/-</sup> mice and their wild-type littermates aged 8–15 weeks, weighing 20–30 g of male and 17–22 g of female mice (supplemental Table I). Mice were housed two per cage in the animal facility of Kyushu University, which was maintained at 21°C, 65% humidity, 12-h light–dark cycle, with *ad libitum* access to food and water.<sup>3</sup>

### Mouse stroke model

Mice were randomly assigned to the animal surgeon, anesthetized by inhalation of 2% isoflurane in air, and maintained on anesthesia using 1.5% isoflurane. Rectal temperatures were maintained at 35–37°C using a heating lamp. Cerebral blood flow before and during ischemia was measured at the ipsilateral parietal bone (2 mm posterior and 4 mm lateral to bregma) using a laser Doppler flowmeter (PeriFlux System 5000, PERIMED, Stockholm, Sweden). Focal cerebral ischemia was induced by pMCAO using a laser-induced photochemical reaction as described previously.<sup>5</sup> The number of mice used in each experiment is shown in Supplemental Table I.

### Behavioral tests

Neurological tests were performed pre-MCAO and 1, 7, 14, 21, and 28 days after MCAO. Motor coordination was evaluated in a quantitative manner using a beam balance test. The apparatus was the surface of an elevated wooden beam ((90 cm (L)  $\times$  2 cm (W)  $\times$  2 cm (H)) at a height of 10 cm from the ground. The number of times that each animal fell off the beam was recorded, and the performance was rated on a scale of 0 to 6 (Supplemental Table II). Three trials were performed on each animal with an interval of 5 min between attempts. The final beam balance score was defined as the mean of the scores received in the three trials.

### Quantitative polymerase chain reaction

Total RNA was isolated from the ischemic area or cultured cells using TRIzol reagent (Thermo Fisher Scientific #15596018, Waltham, MA, USA). Reverse-transcription polymerase chain reaction (PCR) and quantitative real-time PCR were performed as described previously.<sup>5</sup> The mRNA copy numbers were standardized using 18S ribosomal RNA as internal control. Primer sequences are presented in Supplemental Table III.

### Immunoblot analysis

Immunoblot analysis was performed as described previously.<sup>5</sup> Briefly, membranes were incubated at 25°C

for 1 h in ECL Advance blocking reagent (GE Healthcare #RPN418, Chicago, IL, USA) and probed overnight at 4°C with primary antibodies [p-PDGFR $\beta$  (1:500; Cell Signaling Technology (CST) #2227, Boston, MA, USA), PDGFR $\beta$  (1:1000; CST #3169), p-STAT3 (1:1000; CST #9145), STAT3 (1:1000; CST #4904), fibronectin (1:500; BD Biosciences #610077, Franklin Lakes, NJ, USA), laminin  $\alpha$ 2 (1:500; Santa Cruz Biotechnology #sc55605, Dallas, TX, USA), and anti- $\beta$ -actin (1:2,000; Sigma-Aldrich #A5441, St. Louis, MO, USA)]. Membranes were then washed and incubated with secondary antibodies (1:50,000; CST #7074 or #7076) for 45 min at 25°C. Antibodies used are shown in Supplemental Table IV.

### Immunohistochemistry

Mice were euthanized by intraperitoneal administration of pentobarbital (150 mg/kg body weight) and perfused with 4% paraformaldehyde (PFA) in phosphate buffered saline (PBS) at 4°C. After fixing the brain overnight in 4% PFA, 2-mm coronal slices embedded in paraffin were cut into 4- $\mu$ m thick sections. The sections were deparaffinized, rehydrated through a graded series of ethanol solutions, and washed in PBS.<sup>6</sup> After blocking with 5% skimmed milk solution for 30 min at 25°C, sections were incubated with primary antibodies [anti-CD31 (1:200; BD Biosciences #550274), laminin  $\alpha$ 2 (1:500; Santa Cruz Biotechnology #sc59854), laminin  $\alpha$ 4 (1:500; Santa Cruz Biotechnology #sc130541), fibronectin (1:500; BD Biosciences #610077), anti-collagen type IV (1:100; Millipore #AB769, Burlington, MA, USA), anti-perlecan (1:250; Millipore #AB1948P), vitronectin (1:100; Santa Cruz Biotechnology #sc74484), anti-glial fibrillary acidic protein (GFAP) (1:2; DAKO #IS524, Santa Clara, CA, USA), anti-CD13 (1:200; R&D Systems #AF2335, Minneapolis, MN, USA), anti-F4/80 (1:100; Abcam #ab6640, Cambridge, UK), anti-PDGFR $\beta$  (1:200; R&D Systems #AF1042), anti-aquaporin 4 (AQP4) (1:400; Santa Cruz Biotechnology #sc20812), anti-TGF $\beta$ 1 (1:100; Santa Cruz Biotechnology #sc130348), anti-APC (1:100; Millipore #OP80), and anti-Glutathione S-transferase  $\pi$  (GST $\pi$ ) (1:200; MBL #312, Nagoya, Japan)] at 4°C overnight. After washing with PBS/Triton X-100, the sections were incubated with secondary antibodies conjugated to Alexa Fluor dyes (Thermo Fisher Scientific) or stained with 3,3'-diaminobenzidine (Nichirei, Tokyo, Japan). For with 3,3'-diaminobenzidine staining, endogenous peroxidase was inactivated with 0.3% hydrogen peroxide for 30 min before blocking with skim milk solution. EdU (5-ethynyl-2'-deoxyuridine; Thermo Fisher Scientific #A10044) was used to label the proliferating cells to assess oligodendrogenesis. Intraperitoneal EdU injections (50 mg/kg) were administered once daily for 7 days,

beginning on day 1 after pMCAO. Mice were sacrificed on day 28 and perfused with 4% PFA. Brains were removed, 2-mm coronal slices were postfixed for an hour in 4% PFA, and cryoprotected in 30% sucrose overnight. Frozen coronal slices were embedded in optimum cutting temperature compound and sectioned at 4  $\mu$ m. EdU staining was performed using a Click-iTTM EdU imaging kit (Thermo Fisher Scientific #A10338), as described previously.<sup>5</sup> The sections were observed using a BIOREVO BZ-9000 microscope (Keyence, Osaka, Japan) or an inverted confocal microscope (Nikon A1R, Tokyo, Japan). PDGFR $\beta$ , CD13, and fibronectin-positive areas within infarct areas and peri-infarct GFAP- and laminin  $\alpha$ 2-positive areas were obtained in three sections spaced 400  $\mu$ m apart (from bregma +1.0 mm to bregma -0.2 mm). To determine the density of positive cells, three randomly selected squares (200  $\times$  200  $\mu$ m) were analyzed. The density of GST $\pi$ -positive cells in the peri-infarct areas was calculated using three sections spaced 400  $\mu$ m apart (from bregma +1.0 mm to bregma -0.2 mm). To determine the density of positive cells in the peri-infarct areas, four randomly selected squares (400  $\times$  400  $\mu$ m) were analyzed. Ten to 14 animals per group were analyzed.

### Cell culture

Human brain vascular pericytes (#CP1200) were purchased from ScienCell Research Laboratories (Carlsbad, CA, USA) ([https://www.sciencellonline.com/human-brain-vascular-pericyte-cell-pellet.html#product\\_tabs\\_review\\_tabbed](https://www.sciencellonline.com/human-brain-vascular-pericyte-cell-pellet.html#product_tabs_review_tabbed)) and cultured in pericyte medium containing 2% FBS and pericyte growth supplement (#CP1201, ScienCell Research Laboratories). PDGF-BB (10 nM, Wako #16424031), LY364947 (1  $\mu$ M, Wako #123-05981), and stattic (6  $\mu$ M, R&D Systems #19983-44-9)<sup>15</sup> were purchased. Poly-L-lysine (PLL)-coated dishes were purchased from IWAKI (Tokyo, Japan). Bone marrow-derived macrophages (BMDMs) were extracted from male C57BL/6J mice as described previously.<sup>3</sup> Astrocytes, oligodendrocyte precursor cells (OPCs), and microglia were extracted from ICR mice (Japan SLC, Inc) on postnatal day 1, as described previously.<sup>5,16</sup> Cells were cultured in an incubator with 5% CO<sub>2</sub> at 37°C. To investigate the influence of different ECM substrates, culture dishes were coated with a 5  $\mu$ g/mL solution of fibronectin (Sigma-Aldrich #F1141) or laminin 211 (BioLamina AB, Sundbyberg, Sweden), diluted in PBS, overnight at 4°C.

### Immunocytochemistry

Cells were fixed in 4% PFA and processed for immunostaining. They were then incubated for 30 min at

25°C in a blocking solution (5% FBS and 0.3% Triton X-100). The antibodies used to analyze the marker expression profiles were: anti-F4/80 (1:100; Abcam #ab6640), anti-IBA1 (1:500; Abcam #ab5076), anti-MBP (1:500; BioLegend #808401, San Diego, CA, USA), and anti-OLIG2 (1:200; R&D Systems #AF2418). Macrophage phagocytic activity was evaluated using Oil red O (ORO) staining.<sup>3</sup> Fixed cells were dehydrated in 100% propylene glycol for 5 min and stained with 0.5% ORO solution (Sigma-Aldrich #O0625) at 25°C for 15 min. Samples were processed in 85% propylene glycol for 5 min and rinsed with distilled water three times. Stained cells were visualized using an inverted confocal microscope (Nikon A1R, Tokyo, Japan). Cell counting was performed in a blinded manner by randomly selecting four to six fields in each dish.

### *Oxygen and glucose deprivation*

Oxygen glucose deprivation (OGD) was performed using an airtight hypoxia chamber. Cells were washed once with glucose-free Dulbecco's Modified Eagle Medium (DMEM), then subsequently filled with glucose-free DMEM and incubated at 37°C in a humidified atmosphere with 5% CO<sub>2</sub>, 1% O<sub>2</sub>, and 94% N<sub>2</sub> for 24 h.

### *Preparation of myelin debris*

MD was isolated from the brains of 3-month-old mice using sucrose density gradient centrifugation, as described previously.<sup>3</sup> MD was used to stimulate BMDMs and microglia at a concentration of 1 mg/mL myelin protein in all experiments.

### *Preparation of conditioned medium*

BMDM-conditioned medium (MCM) was prepared by first treating the cells for 72 h with DMEM supplemented with 15% conditioned medium from L929 cells and 5% FBS, containing PBS or MD (1 mg/mL). Subsequently, debris was removed from the medium by centrifugation at 200 × g for 5 min. Pericytes were treated with MCM and DMEM at a ratio of 1:2 for 10 min or 24 h. Control medium was prepared using DMEM supplemented with 15% conditioned medium from L929 cells and 5% FBS depleted of BMDMs and DMEM at a ratio of 1:2. Pericyte-conditioned medium (PCM) was prepared by incubating pericytes in minimum pericyte medium containing PBS or platelet-derived growth factor-BB (PDGF-BB) and no growth supplement for 48 h. Subsequently, PCM was collected (referred to as PCM/PBS and PCM/PDGF-BB, respectively). Astrocytes were treated with PCM and DMEM, without serum, at a ratio of

1:1 for 24 h. Control medium was prepared using pericyte medium depleted of cultured pericytes and DMEM at a ratio of 1:1.

### *Adhesion assay*

Cell adhesion assays were performed according to a previously established method.<sup>11</sup> A 96-well cell culture plate was coated with the adhesion molecule overnight at 4°C and blocked with 1% heat-denatured bovine serum albumin at 25°C for 30 min. Cells were preincubated by rotating gently with anti-integrin β1 blocking antibody (BD Biosciences #555003) or control antibody (Armenian Hamster IgM, BD Biosciences #553958) at 50 μg/mL at 37°C for 1 h. Cells were spread at a final concentration of 4 × 10<sup>4</sup> cells/well and incubated at 37°C in 5% CO<sub>2</sub> incubator for 30 min. After washing twice with 0.1% bovine serum albumin in DMEM, cells were fixed with 4% PFA and stained with 0.5% crystal violet (Sigma-Aldrich). The dye was extracted with 2% SDS and the optical density was measured at 590 nm.

### *In vitro OPC differentiation assay*

Primary OPCs were cultured with OPC differentiation medium (N2 medium containing 50 ng/mL of both T3 and T4, Sigma-Aldrich #T2877 and #T2376) on PLL with or without laminin 211 (5 μg/mL)-coated dishes for 5 or 7 days. The medium was replaced every two days.

### *Experimental design and statistical analysis*

Statistical analyses were performed using Prism 8 (GraphPad Software). The Kolmogorov–Smirnov normality test was initially performed on all datasets. The statistical analyses were performed using Student's *t*-tests (for two-group comparisons) and one-way analysis of variance, followed by a post-hoc Bonferroni's comparison test (for multiple group comparisons), as appropriate. All data are presented as mean ± standard deviation. All *p* values <0.05 were considered significant.

## **Results**

### *Post-stroke remodeling of basement membrane ECM proteins*

We examined post-stroke remodeling of ECM that constitute the BM in the intact brain, such as collagen type IV, perlecan, fibronectin, vitronectin, and laminin α2 and α4 in male mice.<sup>9,10</sup> We confirmed that these ECM were localized in the BM surrounding CD31-positive endothelial cells of the intact brain (Figure 1A and Supplemental Figure I). Following pMCAO,

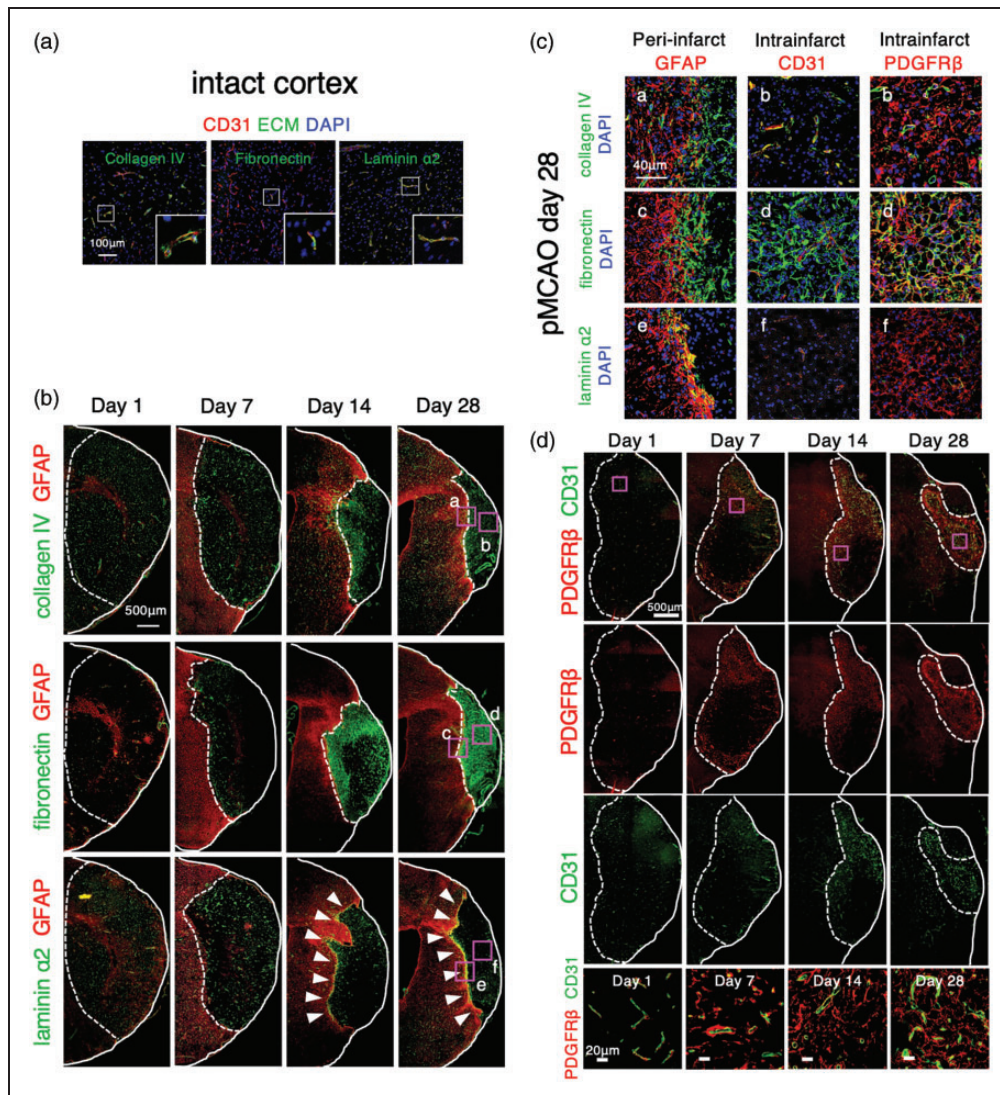


**Figure 1.** Remodeling of extracellular matrix (ECM) proteins after acute ischemic stroke. (a) Immunofluorescent triple labeling of CD31 (red), ECM proteins, either collagen type IV, fibronectin, or laminin  $\alpha 2$  (green), and DAPI (4',6-diamidino-2-phenylindole; blue) in the intact brain of male wild-type mice (scale bar, 100  $\mu\text{m}$ ). Magnified images in the squares are shown in the inset. (b) Immunofluorescent double labeling of GFAP (glial fibrillary acidic protein; red) and ECM, either collagen type IV, fibronectin, or laminin  $\alpha 2$  (green), on day 1, 7, 14, and 28 after permanent middle cerebral artery occlusion (pMCAO) in male wild-type mice (scale bar, 500  $\mu\text{m}$ ). Magnified images of the square in the ischemic border areas (a, c, e) and the ischemic core (b, d, f) on day 28 are shown in (c). Arrowheads show laminin  $\alpha 2$  accumulation in the boundary between infarct areas and peri-infarct astroglia. c, Immunofluorescent triple labeling of GFAP (red), collagen type IV (a), fibronectin (c), or laminin  $\alpha 2$  (e) (green), and DAPI (blue) in peri-infarct area on day 28 after pMCAO in male wild-type mice (scale bar, 40  $\mu\text{m}$ ). Immunofluorescent triple labeling of CD31 or PDGFR $\beta$  (red), collagen type IV (b), fibronectin (d), or laminin  $\alpha 2$  (f) (green), and DAPI (blue) in the ischemic core on day 28 after pMCAO in male wild-type mice (scale bar, 40  $\mu\text{m}$ ) and (d) Immunofluorescent double labeling of CD31 (green) and PDGFR $\beta$  (red) on day 1, 7, 14, and 28 after pMCAO in male wild-type mice (scale bar, 500  $\mu\text{m}$ ). Magnified images in the squares (magenta) are shown at the bottom (scale bar, 20  $\mu\text{m}$ ). PDGFR $\beta$ , platelet-derived growth factor receptor  $\beta$ .

collagen type IV (Figure 1(b) and (c)) and perlecan (Supplemental Figure I) remained localized on small vessel walls surrounding CD31-positive cells within infarct areas and in intact areas (Figure 1(d)), while fibronectin (Figure 1(b) and (c)) and vitronectin (Supplemental Figure I) redistributed gradually within the infarct areas from peri-infarct areas towards

the ischemic core, and eventually occupied the entire infarct areas over 28 days. Their localization was very similar to that of PDGFR $\beta$ , a marker of pericytes, pericyte-derived fibroblast-like cells, and smooth muscle cells (Figure 1(d)). In contrast, perivascular laminin  $\alpha 2$  gradually decreased within infarct areas; instead, it deposited strongly at the boundary between

infarct and peri-infarct areas on day 28 (Figure 1(b) and (c)). Laminin  $\alpha 4$  was localized in infarct areas and peri-infarct areas (Supplemental Figure I).

**PDGFR $\beta$ -positive cells may primarily be responsible for intra-infarct deposition of fibronectin with the aid of neighboring macrophages after pMCAO**

We recently demonstrated that PDGFR $\beta$ -positive pericytes and macrophages play pivotal roles in the clearance of MD and tissue repair within infarct areas through reciprocal interaction (Supplemental Figure II).<sup>3</sup> We therefore examined the expression of fibronectin in cultured BMDMs and pericytes. Quantitative PCR

revealed that fibronectin expression was significantly higher in cultured pericytes than cultured BMDMs at baseline (Figure 2(a)). While OGD did not affect the expression of fibronectin in BMDMs, it significantly increased the expression of fibronectin in cultured pericytes (Figure 2(a)). Furthermore, cultured pericytes showed significantly increased expression of fibronectin in response to PDGF-BB treatment (Figure 2(a)). Macrophages phagocytosing MD increased the expression of *Pdgfrb* and basic fibroblast growth factor (*Fgf2*), an up-regulator of PDGFR $\beta$ <sup>17</sup> (Figure 2(b)). Consistently, MCM treated with MD showed increased phosphorylation of PDGFR $\beta$  and expression of fibronectin in cultured pericytes (Figure 2(c)). We

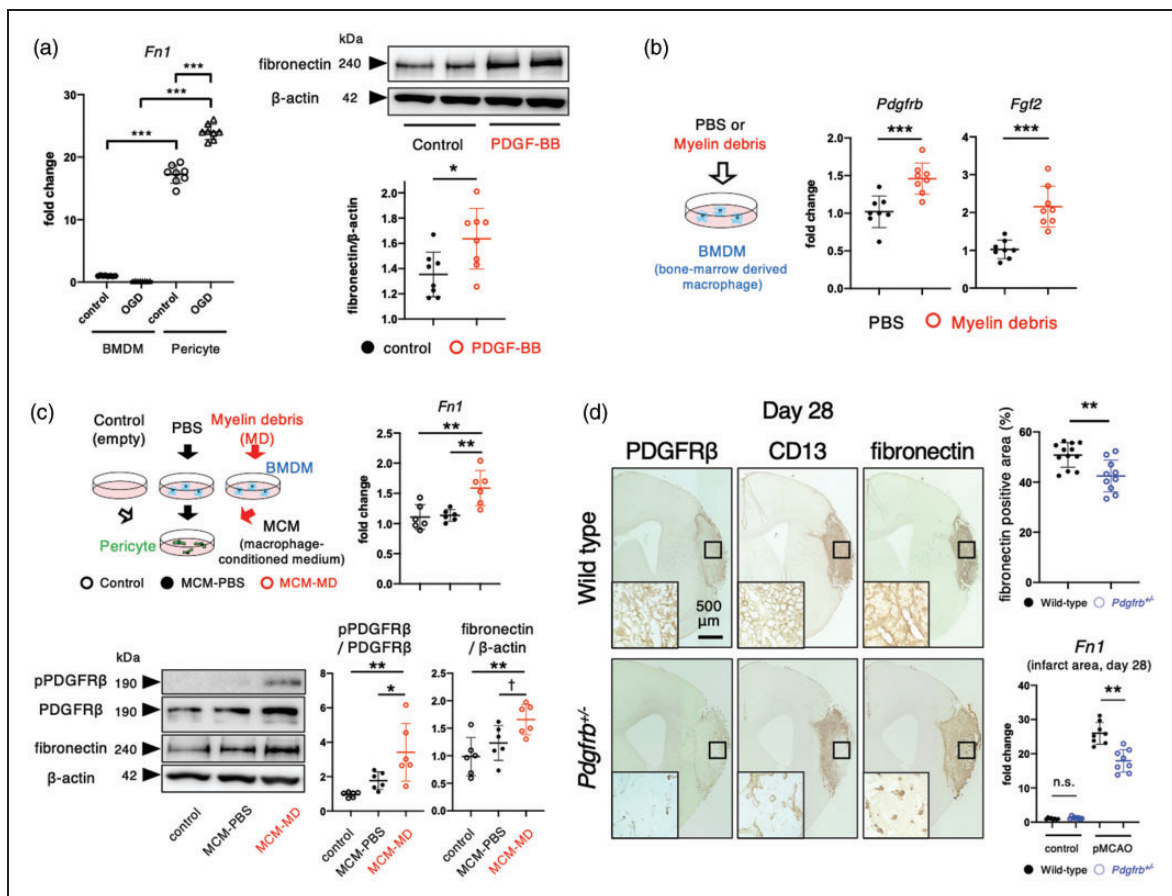


**Figure 2.** PDGFR $\beta$  (platelet-derived growth factor receptor  $\beta$ )-positive pericytes primarily produce fibronectin with the aid of macrophages within infarct areas. (a) Quantitative polymerase chain reaction (PCR) for *Fn1* (fibronectin) in cultured pericytes and bone marrow-derived macrophages (BMDMs) at baseline and after oxygen glucose deprivation for 24 h is shown on the left. Immunoblot analyses of fibronectin and  $\beta$ -actin in cultured pericytes after treatment with PBS or PDGF-BB (10 ng/mL) for 24 h ( $n = 8$ , each group) is shown on the right. (b) Effects of myelin debris (MD) for 72 h on the expression of *Pdgfrb* and *Fgf2* in BMDM ( $n = 8$ ). (c) Effects of macrophage-conditioned medium (MCM) treated with PBS (MCM-PBS) or MD (MCM-MD) for 72 h on PDGFR $\beta$  signaling for 10 min ( $n = 6$ ) and expression changes of *Fn1* mRNA and its protein for 24 h ( $n = 6$ ) in cultured pericytes and (d) Immunohistochemistry of PDGFR $\beta$ , CD13, and fibronectin on day 28 after permanent middle cerebral artery occlusion (pMCAO) in male wild-type and *Pdgfrb*<sup>+/-</sup> mice (scale bar, 500  $\mu$ m) ( $n = 12$ ). Magnified images of ischemic core (black square) are shown in the inset. Quantitative PCR for *Fn1* in the intact brain and in infarct areas on day 28 after pMCAO in male wild-type and *Pdgfrb*<sup>+/-</sup> mice ( $n = 8$ ). Data are shown as mean  $\pm$  standard deviation. a, b, d, \* $p < 0.05$ , \*\* $p < 0.01$ , and \*\*\* $p < 0.001$ ; unpaired  $t$ -test. c, † $p < 0.1$ , \* $p < 0.05$ , and \*\* $p < 0.01$ ; one-way analysis of variance followed by Bonferroni's post-hoc test.

confirmed that MD did not directly affect the phosphorylation of PDGFR $\beta$  and the expression of fibronectin in cultured pericytes (supplemental Figure III). Immunohistochemistry demonstrated that intra-infarct deposition of fibronectin following pMCAO was significantly attenuated in *Pdgfrb*<sup>+/-</sup> mice, wherein post-stroke expression of PDGFR $\beta$  and CD13, another marker of pericytes<sup>18</sup>, was significantly attenuated within infarct areas compared with wild-type mice (Figure 2(d)). Using quantitative PCR, we confirmed that the increased expression of fibronectin in ischemic areas on day 28 after pMCAO was significantly attenuated in *Pdgfrb*<sup>+/-</sup> mice (Figure 2(d)).

### ***Fibronectin enhances the phagocytic activity of macrophages***

We next examined whether fibronectin modulated macrophage functions. Cultured macrophages adhered strongly to fibronectin-coated dishes compared with non-coated ones (control) (Figure 3(a)). Pretreatment with a blocking antibody for integrin  $\beta$ 1 abrogated the adhesion of macrophage to fibronectin (Figure 3(a)). Macrophages cultured on fibronectin-coated dishes showed significantly increased expression of *Il1b*, *Il6*, *Il10*, *Mmp9*, *Tgfb*, and *Msr1*, related to their phagocytic activity and remodeling of ECM. Upregulation of these molecules was significantly attenuated by pretreatment with integrin  $\beta$ 1 antibody (Figure 3(b)). Macrophages cultured on fibronectin-coated dishes showed enhanced phagocytic activity against MD, as assessed by ORO staining (Figure 3(c)), accompanied by increased phosphorylation of STAT3, an indicator of the phagocytic activity of macrophages<sup>19</sup> (Figure 3(d)). Fibronectin-mediated enhancement of phagocytosis was significantly attenuated by stattic, a STAT3 inhibitor<sup>20</sup> (Figures 3(c) and (d)). We further demonstrated that cultured microglia adhered strongly to fibronectin-coated dishes, where they exhibited enhanced phagocytic activity against MD compared with that of microglia on non-coated dishes (control) (Figure 3(e)).

### ***Intra-infarct PDGFR $\beta$ -positive cells promote astrocytic production of laminin $\alpha$ 2 in peri-infarct areas while decreasing their own production of laminin $\alpha$ 2***

In contrast to fibronectin, laminin  $\alpha$ 2 was strongly deposited in the boundary between infarct and peri-infarct areas after pMCAO (Figures 1(b) and (c) and 4(a)). Immunofluorescent labeling demonstrated that peri-infarct laminin  $\alpha$ 2 was co-localized with GFAP (Figure 1(c)) and AQP4, an astrocyte end-feet protein (Figure 4(a)), but not with PDGFR $\beta$  (Figures 1(c) and

4(a)). We further examined the expressional regulation of laminin  $\alpha$ 2 in pericytes and astrocytes. Treatment with PDGF-BB or conditioned medium of macrophages phagocytosing MD (MCM-MD) significantly decreased the expression of laminin  $\alpha$ 2 in cultured pericytes (Figure 4(b)) in contrast to fibronectin (Figure 2). Conversely, PCM treated with PDGF-BB significantly increased the expression of laminin  $\alpha$ 2 in cultured astrocytes (Figure 4(c)). Peri-infarct deposition of laminin  $\alpha$ 2 was significantly attenuated in *Pdgfrb*<sup>+/-</sup> mice, compared with wild-type mice, parallel with the extent of peri-infarct accumulation of GFAP-positive astrocytes (Figure 4(c)). These findings suggest that intra-infarct PDGFR $\beta$ -positive cells crucially regulate the deposition of laminin  $\alpha$ 2 produced by GFAP-positive astrocytes in peri-infarct areas through humoral factors.

We then explored whether PDGFR $\beta$ -positive cell-derived molecules could upregulate the expression of laminin  $\alpha$ 2 in peri-infarct astrocytes. Among all candidates, we focused on transforming growth factor  $\beta$ 1 (TGF $\beta$ 1) and interleukin-6 (IL-6) because these two molecules were expressed in cultured PDGFR $\beta$ -positive pericytes and their expression was significantly increased in response to PDGF-BB (Figure 4(d)). Treatment with TGF $\beta$ 1, but not with IL-6, significantly increased the expression of laminin  $\alpha$ 2 in cultured astrocytes (Figure 4(d)). Pretreatment with LY364947 (1  $\mu$ M), a TGF $\beta$ 1 receptor inhibitor, significantly attenuated the upregulation of laminin  $\alpha$ 2 induced by PCM (treated with PDGF-BB) in the cultured astrocytes (Figure 4(c)). Consistently, TGF $\beta$ 1, which was expressed partly in PDGFR $\beta$ -positive cells, was markedly increased within infarct areas, but significantly decreased in *Pdgfrb*<sup>+/-</sup> mice (Figure 4(d)).

We further examined the possibility whether peri-infarct laminin  $\alpha$ 2 can also function as a glial limitans against macrophages. Cultured macrophages did not adhere to laminin  $\alpha$ 2 (laminin 211)-coated dishes (Figure 4(e)). Macrophages cultured on laminin  $\alpha$ 2-coated dishes showed reduced expression of *Pdgfb*, *Fgf2*, *Il1b*, and *Il6* (Figure 4(e)). Moreover, the adherence of cultured microglia was reduced on laminin  $\alpha$ 2-coated dishes (Figure 3(e)). In *Pdgfrb*<sup>+/-</sup> mice, more F4/80-positive cells infiltrated into GFAP-positive peri-infarct areas, probably due to reduced deposition of laminin  $\alpha$ 2 at the infarct boundary (Figure 4(e)).

### ***Peri-infarct laminin $\alpha$ 2 may promote oligodendrogenesis, a key process for functional recovery***

Finally, we examined the effects of laminin  $\alpha$ 2 on the oligodendrogenesis in peri-infarct areas, a key process promoting post-stroke functional recovery.<sup>5,21</sup>

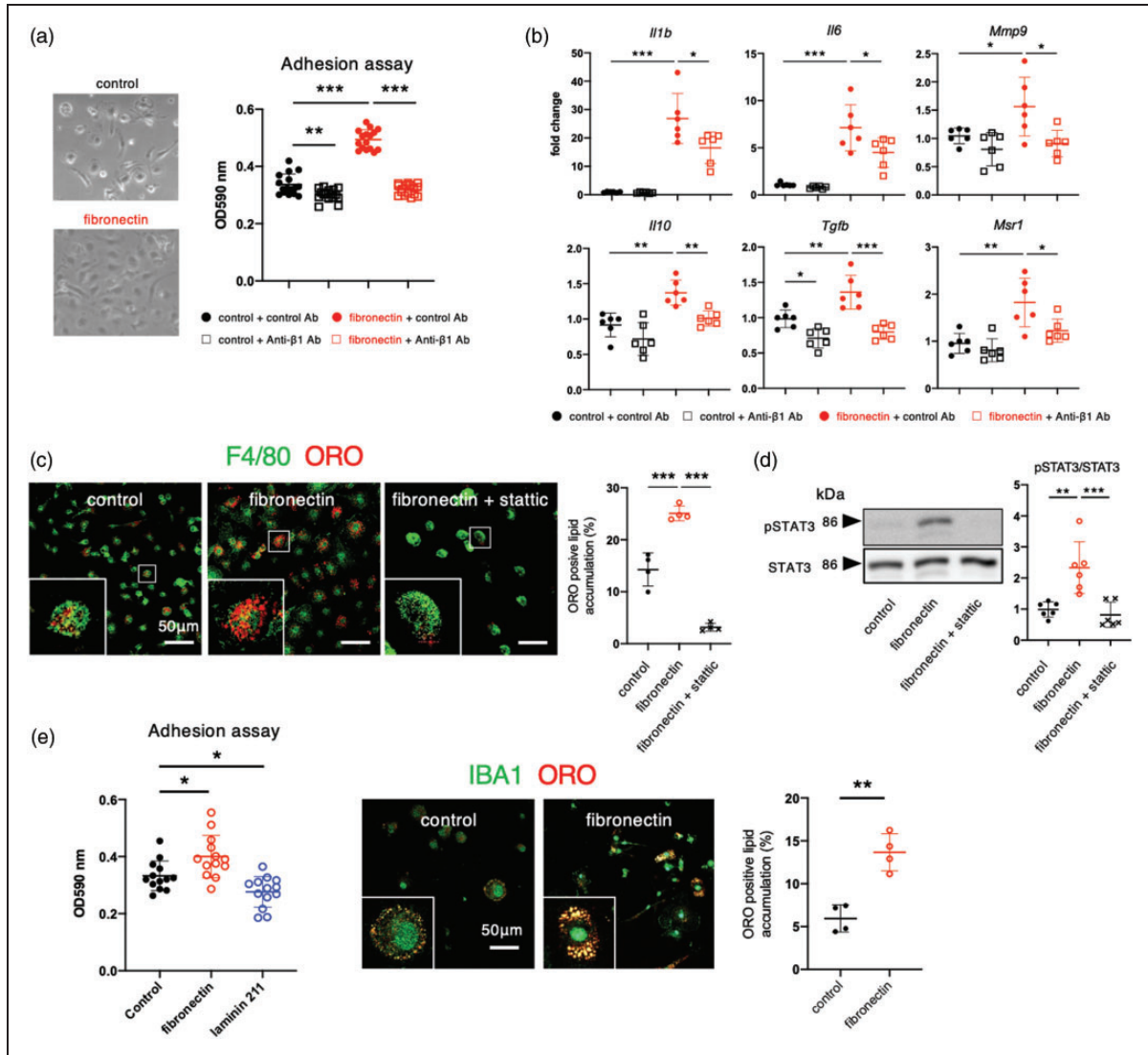


**Figure 3.** Fibronectin enhances the activity of macrophages within infarct areas. (a) Representative images of bone marrow-derived macrophages (BMDMs) cultured on non-coated (control) and fibronectin-coated dishes. Adhesion of BMDMs to fibronectin is attenuated by co-treatment with an anti-integrin β1 antibody (50 mg/mL). (b) Quantitative polymerase chain reaction for *Il1b*, *Il6*, *Mmp9*, *Il10*, *Tgfb*, and *Msr1* in BMDMs cultured on control or fibronectin-coated dish with or without an anti-integrin β1 antibody for 6 h (n = 6). (c) Immunofluorescent assessment of phagocytotic activity of BMDM for myelin debris (MD). Immunofluorescent double labeling with F4/80 (green) and Oil Red O (ORO) (red) in BMDMs cultured on control, fibronectin-coated, or fibronectin-coated dish with stattic (6 μmol/L) for 24 h. Quantification of ORO-positive (red) foamy macrophages is shown on the right (n = 4). Magnified images are shown in the inset: F4/80-positive macrophages (green) took up MD and became ORO-positive (red) foamy macrophages in 24 h. (d) Representative immunoblot analyses of total STAT3 (signal transducer and activator of transcription 3) and phosphorylated STAT3 in BMDMs cultured on control, fibronectin-coated, and fibronectin-coated dishes with stattic (6 μmol/L) (n = 6) and (e) Adhesion of cultured microglia on non-coated (control), fibronectin-coated, and laminin α2-coated dishes (n = 13). Assessment of phagocytotic activity of cultured microglia for MD. Immunofluorescent double labeling with F4/80 (green) and ORO (red) in microglia cultured on control and fibronectin-coated dishes for 24 h. Data are shown as mean ± standard deviation. \*p < 0.05, \*\*p < 0.01, and \*\*\*p < 0.001; one-way analysis of variance followed by Bonferroni's post-hoc test.

In contrast to macrophages, cultured OPCs adhered well to laminin α2 (laminin 211)-coated dishes (Figure 5(a)). Quantitative PCR revealed that OPCs showed increased expression of myelinating proteins, such as *Mbp*, *Mag*, and *Plp*, on laminin α2 (laminin 211)-coated dishes (Figure 5(a)). Consistently,

immunofluorescent labeling showed increased expression of MBP in OLIG2-positive OPCs cultured on laminin α2-coated dishes (Figure 5(b)). Immunofluorescent triple labeling demonstrated that some APC-positive oligodendrocytes were EdU-positive close to laminin α2-positive peri-infarct areas, suggesting that the



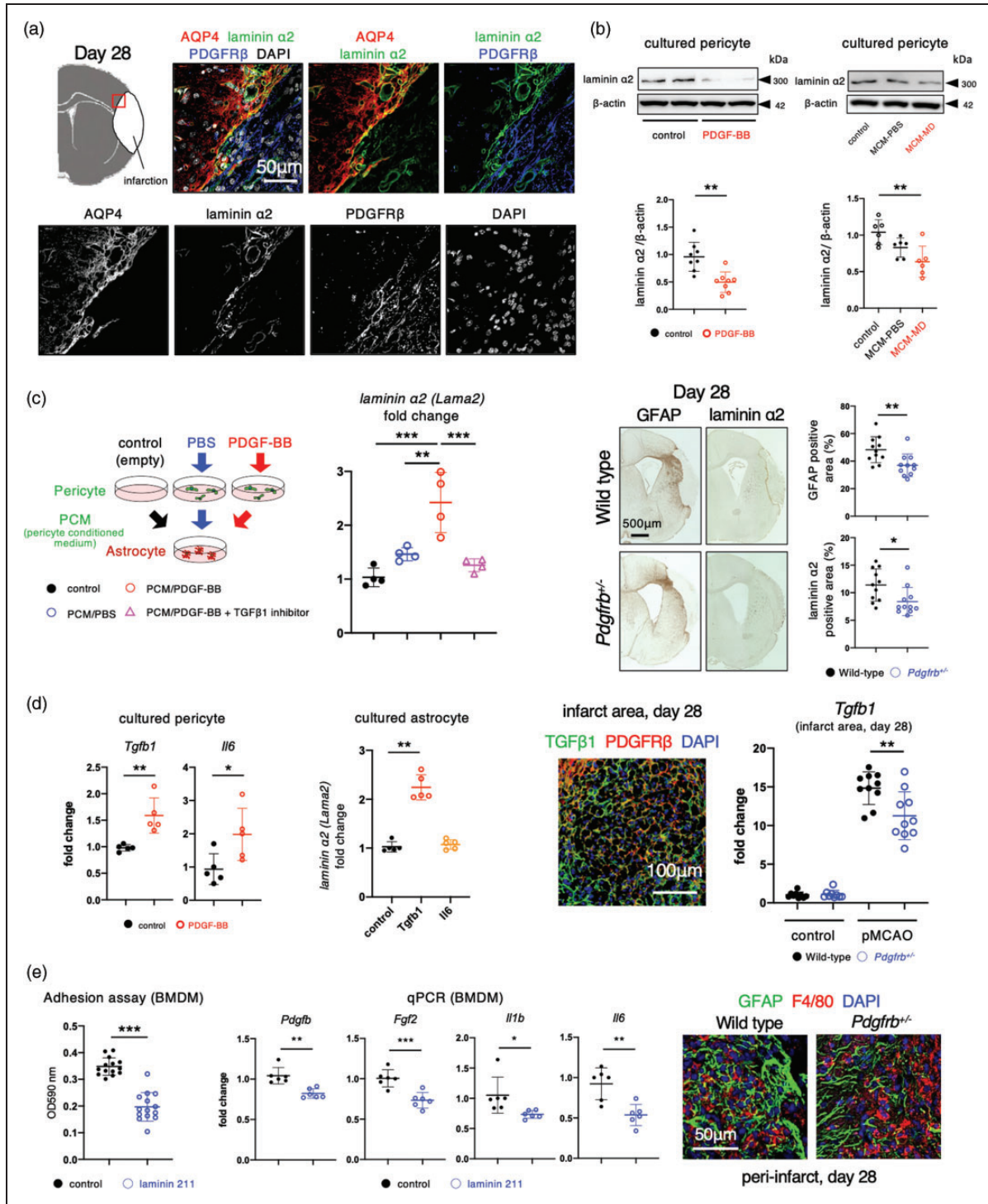


**Figure 4.** Intra-infarct PDGFR $\beta$  (platelet-derived growth factor receptor  $\beta$ )-positive cells promote astrocytic production of laminin  $\alpha 2$  in peri-infarct areas. a, Immunofluorescent quadruple labeling with DAPI (4',6-diamidino-2-phenylindole; white), AQP4 (aquaporin 4, red), laminin  $\alpha 2$  (green), and PDGFR $\beta$  (blue) in peri-infarct areas on day 28 after permanent middle cerebral artery occlusion (pMCAO) (scale bar, 50  $\mu$ m). The peri-infarct region (red square) in the top-left panel is magnified. b, Immunoblot analyses of laminin  $\alpha 2$  and  $\beta$ -actin in cultured pericytes after treatment with PBS or PDGF-BB (10 ng/mL) for 24 h (n = 8, each group) (left). Effects of macrophage-conditioned medium (MCM) treated with PBS (MCM-PBS) or myelin debris (MCM-MD) on expression changes of laminin  $\alpha 2$  in cultured pericytes (n = 6). c, Effects of pericyte-conditioned medium (PCM) (black, control) and PCM treated with PBS (blue, PCM/PBS) or PDGF-BB (10 ng/mL; red, PCM/PDGF-BB) on the expression of laminin  $\alpha 2$  in cultured astrocytes. Effect of LY364947 (1  $\mu$ M), an inhibitor of TGF $\beta$ 1 receptor, was tested (n = 4) (left). Immunohistochemistry of GFAP (glial fibrillary acidic

Continued.

oligodendrocytes were generated from OPCs in these areas (Figure 5(c)). The number of peri-infarct GST $\pi$ -positive oligodendrocytes was significantly lower in *Pdgfrb*<sup>+/-</sup> mice than wild-type mice (Figure 5(c)). We demonstrated that post-stroke functional recovery was significantly attenuated in *Pdgfrb*<sup>+/-</sup> mice (Figure 5(d)).

We further confirmed that post-stroke deposition of intra-infarct fibronectin and peri-infarct laminin  $\alpha$ 2 and OPC differentiation, as assessed by GST $\pi$ , were decreased with worse functional recovery in female *Pdgfrb*<sup>+/-</sup> mice (supplemental Figure IV).

## Discussion

We demonstrated that ECMs constituting the BM in the intact brain were drastically remodeled after acute ischemic stroke: some ECMs, such as collagen type IV and perlecan, remained in the BM surrounding residual endothelial cells within infarct areas,<sup>11</sup> while others were remodeled to infarct areas in parallel with accumulation of PDGFR $\beta$ -positive cells (fibronectin and vitronectin)<sup>22</sup> or to peri-infarct areas (laminin  $\alpha$ 2).<sup>23</sup> Among them, we focused on fibronectin and laminin  $\alpha$ 2 in the present study. Fibronectin, chiefly produced by PDGFR $\beta$ -positive cells with the aid of macrophages within infarct areas, enhanced macrophage-mediated clearance of MD and tissue repair within infarct areas. In contrast, laminin  $\alpha$ 2 may demarcate the infarct border and function as a promoter of oligodendrogenesis in peri-infarct areas. Since the peri-infarct deposition of laminin  $\alpha$ 2 was reduced in *Pdgfrb*<sup>+/-</sup> mice, intra-infarct PDGFR $\beta$ -positive cells may organize the post-stroke remodeling of these ECM.

### PDGFR $\beta$ -positive cell-derived fibronectin is a key ECM promoting macrophage-mediated clearance of debris within infarct areas

Fibronectin can be produced by various cell types including pericytes/fibroblasts,<sup>22</sup> astrocytes,<sup>24</sup> and microglia/macrophages.<sup>25</sup> However, the present study clearly demonstrated that PDGFR $\beta$ -positive cells may

primarily be responsible for the production of fibronectin within infarct areas, based on the following findings: (1) fibronectin was deposited gradually within infarct areas in parallel with intra-infarct accumulation of PDGFR $\beta$ -positive cells following pMCAO<sup>3</sup>; (2) fibronectin deposition was significantly reduced in *Pdgfrb*<sup>+/-</sup> mice; and (3) quantitative PCR demonstrated that the expression levels of fibronectin were much higher in cultured PDGFR $\beta$ -positive pericytes than macrophages, another major cell type within infarct areas.<sup>3</sup> Infiltrating macrophages contribute to the PDGFR $\beta$ -positive cell-mediated production of fibronectin, which enhances macrophage activity, such as adhesion, gene expression, and clearance of MD. Thus, fibronectin may mediate close interaction between PDGFR $\beta$ -positive cells and macrophages, thereby completing the clearance of debris within infarct areas.<sup>3</sup> Reportedly, fibronectin plays an important role in mediating axonal regeneration.<sup>24,26</sup> Additionally, we and others have demonstrated recently that effective intra-infarct tissue repair promotes peri-infarct astrogliosis and oligodendrogenesis leading to better functional recovery.<sup>3,5</sup> Collectively, fibronectin produced by PDGFR $\beta$ -positive cells may be a key ECM promoting post-stroke functional recovery through enhancement of macrophage-mediated debris clearance within infarct areas. In this context, we suppose that attenuated deposition of intra-infarct fibronectin and peri-infarct laminin  $\alpha$ 2 in *Pdgfrb*<sup>+/-</sup> mice are attributable chiefly to phenotypic changes of pericytes and pericyte-derived fibroblast-like cells<sup>5,7,27,28</sup>; however, we could not exclude the possibility that vascular smooth muscles and/or non-pericyte-derived fibroblast-like cells also contribute to the altered ECM deposition because these cells can also express PDGFR $\beta$ .

In addition to BMDMs infiltrating into infarct areas, resident microglia may also play roles in the clearance of MD in ischemic areas and post-injury functional recovery, since cultured microglia also adhered strongly to fibronectin-coated dishes, thereby enhancing their phagocytic activity against MD.<sup>29</sup>

#### Figure 4. Continued.

protein) and laminin  $\alpha$ 2 on day 28 after pMCAO in male wild-type and *Pdgfrb*<sup>+/-</sup> mice (scale bar, 500 mm). Quantitative data are shown on the right (n = 10). (d) Expression of *Tgfb1* and *Il6* in cultured pericytes and their expression changes in response to PDGF-BB (n = 5) (left). Effects of TGF $\beta$ 1 and IL-6 on the expression of laminin  $\alpha$ 2 in cultured astrocytes (n = 5) (middle). Immunofluorescent triple labeling with TGF $\beta$ 1 (green), PDGFR $\beta$  (red), and DAPI (blue) in infarct areas on day 28 after pMCAO (scale bar, 100 mm). Expression of *Tgfb1* mRNA in intact areas at day 0 (control) and that within infarct areas at day 28 after pMCAO in wild-type and *Pdgfrb*<sup>+/-</sup> mice (n = 10) and (e) Adhesion of bone marrow-derived macrophages (BMDMs) to non-coated (control) or laminin  $\alpha$ 2 (laminin 211)-coated dishes (left). Quantitative polymerase chain reaction for *Pdgfb*, *Fgf2*, *Il1b*, and *Il6* in BMDMs on control or laminin  $\alpha$ 2 (laminin 211)-coated dishes (middle). Representative immunofluorescent triple labeling with GFAP (green), F4/80 (red), and DAPI (blue) on day 28 after pMCAO in male wild-type and *Pdgfrb*<sup>+/-</sup> mice (scale bar, 50 mm) (right). Data are shown as mean  $\pm$  standard deviation. (b) \*p < 0.05, \*\*p < 0.01, and \*\*\*p < 0.001; one-way analysis of variance followed by Bonferroni's post-hoc test. (c–e) \*p < 0.05, \*\*p < 0.01, and \*\*\*p < 0.001; unpaired t-test.

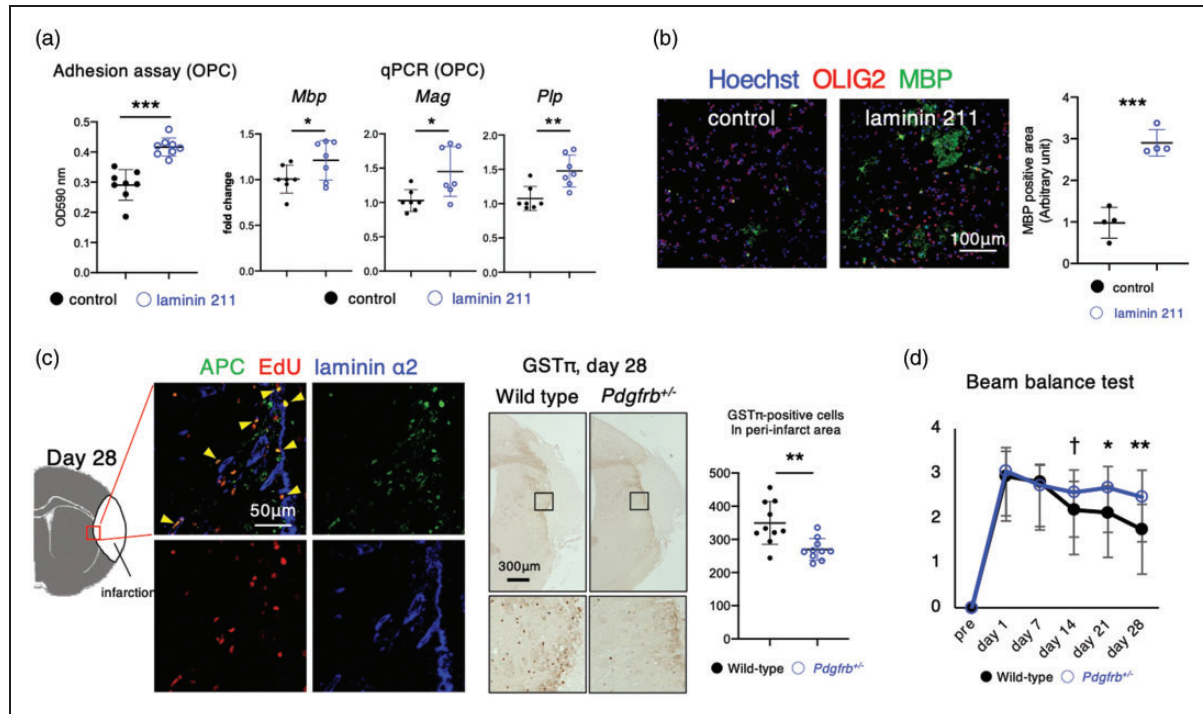


**Figure 5.** Laminin  $\alpha 2$  promotes oligodendrogenesis, a key process of functional recovery, in peri-infarct areas. (a) Adhesion of oligodendrocyte precursor cells (OPCs) to non-coated (control) or laminin  $\alpha 2$  (laminin 211)-coated dishes. Quantitative polymerase chain reaction of myelin basic protein (*Mbp*), myelin-associated glycoprotein (*Mag*), and myelin proteolipid protein (*Plp*) in OPCs cultured on control or laminin  $\alpha 2$  (laminin 211)-coated dishes for 5 days ( $n = 7$ ). (b) Representative immunofluorescent triple labeling of Hoechst (blue), MBP (green), and OLIG2 (oligodendrocyte lineage transcription factor 2; red) in OPCs cultured on control or laminin  $\alpha 2$  (laminin 211)-coated dishes for 7 days ( $n = 4$ ; scale bar, 100  $\mu\text{m}$ ), and quantification of the MBP-positive areas. (c) Representative immunofluorescent triple labeling with laminin  $\alpha 2$  (blue), APC (adenomatous polyposis coli, green), and EdU (5-ethynyl-2'-deoxyuridine, red) in peri-infarct areas (red square) on day 28 after permanent middle cerebral artery occlusion (pMCAO) in male wild-type mice (scale bar, 50  $\mu\text{m}$ ) (left). Immunohistochemistry of GST $\pi$  (glutathione S-transferase  $\pi$ ) on day 28 after pMCAO in male wild-type and *Pdgfrb*<sup>+/-</sup> mice (scale bar, 300  $\mu\text{m}$ ) ( $n = 10$ ) (right) and (d) Neurological function, assessed using the beam balance test, at baseline (Pre) and at days 1, 7, 14, 21, and 28 after pMCAO in male wild-type (black;  $n = 16$ ) and *Pdgfrb*<sup>+/-</sup> mice (blue;  $n = 17$ ). Data are shown as mean  $\pm$  standard deviation. † $p < 0.1$ , \* $p < 0.05$ , \*\* $p < 0.01$ , and \*\*\* $p < 0.001$ ; unpaired  $t$ -test.

### PDGFR $\beta$ -positive cells regulate the production of astrocytic laminin $\alpha 2$ in peri-infarct areas

Laminin  $\alpha 2$  can be produced by pericytes and astrocytes and is a key ECM<sup>14,23,30</sup> that restricts the extravasation of blood-derived monocytes/macrophages into the brain parenchyma in the BBB.<sup>31</sup> Within infarct areas, (1) astrocytes are lost; (2) PDGFR $\beta$ -positive pericytes decrease the expression of laminin  $\alpha 2$  in response to PDGF-BB or MCM; and (3) infiltrating macrophages, along with pericytes,<sup>32</sup> produce MMP9, a metalloproteinase preferentially degrading laminin  $\alpha 2$ .<sup>33,34</sup> Therefore, the BM laminin  $\alpha 2$  is reduced within infarct areas, as shown in the present study. In contrast to reduced expression of laminin  $\alpha 2$  within infarct areas, it was produced by peri-infarct GFAP-positive astrocytes and deposited strongly in the boundary between infarct and peri-infarct areas. Since pericyte-conditioned media increased the

production of laminin  $\alpha 2$  in cultured astrocytes and the deposition of laminin  $\alpha 2$  was significantly attenuated in *Pdgfrb*<sup>+/-</sup> mice, intra-infarct PDGFR $\beta$ -positive cells may crucially regulate the laminin  $\alpha 2$  production in peri-infarct astrocytes probably through humoral factors. In this context, we identified TGF $\beta 1$  as a candidate molecule produced by PDGFR $\beta$ -positive cells, which could increase the expression of laminin  $\alpha 2$  in peri-infarct GFAP-positive astrocytes (Figure 4(d)). However, to prove this in vivo, we should examine whether post-stroke deposition of laminin  $\alpha 2$  in peri-infarct areas would be decreased in mice with PDGFR $\beta$ -positive cell-specific deletion of *Tgfb1*.

### Astrocytic laminin $\alpha 2$ may function as a promotor of oligodendrogenesis in peri-infarct areas

Peri-infarct astrocytic laminin  $\alpha 2$  may have important roles after ischemic stroke. It may promote peri-infarct

oligodendrogenesis/remyelination, leading to functional recovery. We have recently demonstrated that effective intra-infarct repair promotes peri-infarct oligodendrogenesis and astrogliosis.<sup>5</sup> Furthermore, various molecules produced by astrocytes promote oligodendrogenesis;<sup>5,21,35</sup> laminin  $\alpha 2$  may be one such factor as it functions as a scaffold for OPCs for differentiation into oligodendrocytes in peri-infarct areas. Previous reports have demonstrated that the deficiency of laminin  $\alpha 2$  causes developmental abnormality of OPC differentiation, thereby leading to myelination defects in both humans<sup>36</sup> and animals.<sup>37</sup> Reportedly, pericytes directly stimulated OPC differentiation and remyelination through the production of laminin  $\alpha 2$  in a mouse demyelination model using *Pdgfrb*-deficient mice.<sup>38</sup> However, at least in acute ischemic stroke, PDGFR $\beta$ -positive pericytes may indirectly stimulate peri-infarct OPC differentiation through astrocyte-mediated production of laminin  $\alpha 2$ .

## Limitations

This study has certain limitations. First, we did not examine post-stroke remodeling of all ECM components in the brain. There may be more interesting ECM, besides fibronectin and laminin  $\alpha 2$ , that crucially affect post-stroke tissue repair and functional recovery. Second, we should confirm the *in vivo* role of fibronectin and laminin  $\alpha 2$  using mice with pericyte-specific deletion of fibronectin or astrocyte-specific deletion of laminin  $\alpha 2$ , although Yao et al. demonstrated that deficiency of astrocytic laminin causes instability of the BBB *in vivo*.<sup>23</sup> Finally, we only used young mice. Aged mice or those with risk factors for stroke should be used to examine the effects of PDGFR $\beta$  deficiency on post-stroke remodeling of ECM. Bell et al. demonstrated that pericytic dysfunctions become greater with aging in *Pdgfrb*<sup>+/-</sup> mice<sup>39</sup>; therefore, we speculate that post-stroke ECM remodeling may be impaired more in aged *Pdgfrb*<sup>+/-</sup> mice.

In conclusion, intra-infarct PDGFR $\beta$ -positive cells organize post-stroke remodeling of ECM, like fibronectin and laminin  $\alpha 2$ , thereby promoting tissue repair and functional recovery following acute ischemic stroke. These ECM can be therapeutic targets for post-stroke functional recovery.

## Funding

The author(s) disclosed receipt of the following financial support for the research, authorship, and/or publication of this article: This work was supported by Grants-in-Aid for Scientific Research (B 16H05439), (B 20H03791) (TK and TA), (C 20K09373) (TA), (C 26462163), (GAG9K09530) (YW), and (C GAG9K09511) (KN) from the Ministry of Education, Culture, Sports, Science and Technology, Japan;

a grant from Mochida Memorial Foundation for Medical and Pharmaceutical Research (KN); a grant from SENSHIN Medical Research Foundation, Japan (TA and KN); a grant from the Smoking Research Foundation (TA); and research grants from Boehringer Ingelheim, Bristol-Myers Squibb, Daiichi Sankyo, Eisai, and Takeda (TK and TA).

## Acknowledgements

We thank Naoko Kasahara and Hideko Noguchi (Kyushu University) for technical support and Keiko Hirano (Kyushu University) for secretarial assistance. We also thank Editage ([www.editage.com](http://www.editage.com)) for English language editing.

## Declaration of conflicting interests

The author(s) declared no potential conflicts of interest with respect to the research, authorship, and/or publication of this article.

## Authors' contributions

TS, KN, YW, and TA contributed to the conception and design of the study; TS, MS, KY, MT HT, and MH contributed to the acquisition and analysis of data; TS and TA contributed to drafting the manuscript; and TS, KN, YW, TK, and TA contributed to revising the manuscript.

## ORCID iDs

Masahiro Shijo  <https://orcid.org/0000-0001-6851-2860>  
Tetsuro Ago  <https://orcid.org/0000-0003-4560-6594>

## Supplemental material

Supplemental material for this article is available online.

## References

1. National institute of neurological disorders and stroke rt-PA stroke study group. Tissue plasminogen activator for acute ischemic stroke. *N Engl J Med* 1995; 333: 1581–1587.
2. Goyal M, Menon BK, van Zwam WH, HERMES orators, et al. Endovascular thrombectomy after large-vessel ischaemic stroke: a meta-analysis of individual patient data from five randomised trials. *Lancet* 2016; 387: 1723–1731.
3. Shibahara T, Ago T, Tachibana M, et al. Reciprocal interaction between pericytes and macrophage in post-stroke tissue repair and functional recovery. *Stroke* 2020; 51: 3095–3106.
4. Ting SM, Zhao X, Sun G, et al. Brain cleanup as a potential target for poststroke recovery: the role of RXR (retinoic X receptor) in phagocytes. *Stroke* 2020; 51: 958–966.
5. Shibahara T, Ago T, Nakamura K, et al. Pericyte-mediated tissue repair through PDGFR $\beta$  promotes peri-infarct astrogliosis, oligodendrogenesis, and functional recovery after acute ischemic stroke. *eNeuro* 2020; 7: ENEURO.0474-0419.2020.

6. Tachibana M, Ago T, Wakisaka Y, et al. Early reperfusion after brain ischemia has beneficial effects beyond rescuing neurons. *Stroke* 2017; 48: 2222–2230.
7. Caplan AI and Correa D. The MSC: an injury drugstore. *Cell Stem Cell* 2011; 9: 11–15.
8. Amruta N, Rahman AA, Pinteaux E, et al. Neuroinflammation and fibrosis in stroke: the good, the bad and the ugly. *J Neuroimmunol* 2020; 346: 577318.
9. Stratman AN, Malotte KM, Mahan RD, et al. Pericyte recruitment during vasculogenic tube assembly stimulates endothelial basement membrane matrix formation. *Blood* 2009; 114: 5091–5101.
10. Roberts J, Kahle MP and Bix GJ. Perlecan and the blood-brain barrier: beneficial proteolysis? *Front Pharmacol* 2012; 3: 155.
11. Nakamura K, Ikeuchi T, Nara K, et al. Perlecan regulates pericyte dynamics in the maintenance and repair of the blood-brain barrier. *J Cell Biol* 2019; 218: 3506–3525.
12. Di Russo J, Hannocks MJ, Luik AL, et al. Vascular laminins in physiology and pathology. *Matrix Biol* 2017; 57–58: 140–148.
13. Gautam J, Zhang X and Yao Y. The role of pericytic laminin in blood brain barrier integrity maintenance. *Sci Rep* 2016; 6: 36450.
14. Kang M and Yao Y. Basement membrane changes in ischemic stroke. *Stroke* 2020; 51: 1344–1352.
15. Schust J, Sperl B, Hollis A, et al. Stattic: a small-molecule inhibitor of STAT3 activation and dimerization. *Chem Biol* 2006; 13: 1235–1242.
16. Sekine N, Yokota S and Oshio S. Sperm morphology is different in two common mouse strains. *BPB Reports* 2021; 4: 162–165.
17. Nakamura K, Arimura K, Nishimura A, et al. Possible involvement of basic FGF in the upregulation of PDGFR $\beta$  in pericytes after ischemic stroke. *Brain Res* 2016; 1630: 98–108.
18. Smyth LCD, Rustenhoven J, Scotter EL, et al. Markers for human brain pericytes and smooth muscle cells. *J Chem Neuroanat* 2018; 92: 48–60.
19. Campana L, Starkey Lewis PJ, Pellicoro A, et al. The STAT3-IL-10-IL-6 pathway is a novel regulator of macrophage efferocytosis and phenotypic conversion in sterile liver injury. *J Immunol* 2018; 200: 1169–1187.
20. Balanis N, Wendt MK, Schiemann BJ, et al. Epithelial to mesenchymal transition promotes breast cancer progression via a fibronectin-dependent STAT3 signaling pathway. *J Biol Chem* 2013; 288: 17954–17967.
21. Zhang R, Chopp M and Zhang ZG. Oligodendrogenesis after cerebral ischemia. *Front Cell Neurosci* 2013; 7: 201.
22. Makihara N, Arimura K, Ago T, et al. Involvement of platelet-derived growth factor receptor  $\beta$  in fibrosis through extracellular matrix protein production after ischemic stroke. *Exp Neurol* 2015; 264: 127–134.
23. Yao Y, Chen ZL, Norris EH, et al. Astrocytic laminin regulates pericyte differentiation and maintains blood brain barrier integrity. *Nat Commun* 2014; 5: 3413.
24. Tom VJ, Doller CM, Malouf AT, et al. Astrocyte-associated fibronectin is critical for axonal regeneration in adult white matter. *J Neurosci* 2004; 24: 9282–9290.
25. Tsukamoto Y, Hessel WE and Wahl SM. Macrophage production of fibronectin, a chemoattractant for fibroblasts. *J Immunol* 1981; 127: 673–678.
26. Yanqing Z, Yu-Min L, Jian Q, et al. Fibronectin and neuroprotective effect of granulocyte colony-stimulating factor in focal cerebral ischemia. *Brain Res* 2006; 1098: 161–169.
27. Goritz C, Dias DO, Tomilin N, et al. A pericyte origin of spinal cord scar tissue. *Science* 2011; 333: 238–242.
28. Winkler EA, Bell RD and Zlokovic BV. Pericyte-specific expression of PDGF beta receptor in mouse models with normal and deficient PDGF beta receptor signaling. *Mol Neurodegener* 2010; 5: 32.
29. Milner R and Campbell IL. Cytokines regulate microglial adhesion to laminin and astrocyte extracellular matrix via protein kinase C-dependent activation of the alpha6beta1 integrin. *J Neurosci* 2002; 22: 1562–1572.
30. Armulik A, Genové G, Mäe M, et al. Pericytes regulate the blood-brain barrier. *Nature* 2010; 468: 557–561.
31. Voisin MB, Woodfin A and Nourshargh S. Monocytes and neutrophils exhibit both distinct and common mechanisms in penetrating the vascular basement membrane in vivo. *Arterioscler Thromb Vasc Biol* 2009; 29: 1193–1199.
32. Nishimura A, Ago T, Kuroda J, et al. Detrimental role of pericyte Nox4 in the acute phase of brain ischemia. *J Cereb Blood Flow Metab* 2016; 36: 1143–1154.
33. Gu Z, Cui J, Brown S, et al. A highly specific inhibitor of matrix metalloproteinase-9 rescues laminin from proteolysis and neurons from apoptosis in transient focal cerebral ischemia. *J Neurosci* 2005; 25: 6401–6408.
34. Yao Y. Basement membrane and stroke. *J Cereb Blood Flow Metab* 2019; 39: 3–19.
35. Miyamoto N, Maki T, Shindo A, et al. Astrocytes promote oligodendrogenesis after white matter damage via brain-derived neurotrophic factor. *J Neurosci* 2015; 35: 14002–14008.
36. Allamand V and Guicheney P. Merosin-deficient congenital muscular dystrophy, autosomal recessive (MDC1A, MIM#156225, LAMA2 gene coding for  $\alpha 2$  chain of laminin). *Eur J Hum Genet* 2002; 10: 91–94.
37. Relucio J, Menezes MJ, Miyagoe-Suzuki Y, et al. Laminin regulates postnatal oligodendrocyte production by promoting oligodendrocyte progenitor survival in the subventricular zone. *Glia* 2012; 60: 1451–1467.
38. De La Fuente AG, Lange S, Silva ME, et al. Pericytes stimulate oligodendrocyte progenitor cell differentiation during CNS remyelination. *Cell Rep* 2017; 20: 1755–1764.
39. Bell RD, Winkler EA, Sagare AP, et al. Pericytes control key neurovascular functions and neuronal phenotype in the adult brain and during brain aging. *Neuron* 2010; 68: 409–427.